THE AMERICAN SOCIETY OF MECHANICAL ENGINEERS
345 E. 47th St., New York, N.Y. 10017

97-GT-238

THEORY AND METHODOLOGY OF OPTIMALLY MEASURING VIBRATORY STRAINS IN CLOSELY SPACED MODES

M.-T. Yang and **J.H. Griffin**
Department of Mechanical Engineering
Carnegie Mellon University
Pittsburgh, Pennsylvania

ABSTRACT

Stress ratios are traditionally used to infer maximum stresses in blades from strain measurements. This method may not be applicable to all the modes of modern low aspect ratio (LAR) blades since LAR blades often have high frequency "tip" modes which are so closely spaced that slight changes in structural properties can cause significant mode shape changes.

In this paper, it is first shown that the actual tip modes of a LAR blade can be well approximated as linear combinations of the "nominal" modes. The stress field of the blade can then be estimated by calculating the modal content from multiple strain measurements. However, since placement and gage inaccuracies can introduce significant errors in the calculation, it is necessary to find the optimal gage placement which minimizes the error in estimated stresses. An error estimate using "norms" and an efficient optimization method are developed for this purpose.

1. INTRODUCTION

Stress ratios and strain gage measurements are frequently used to infer the maximum stress in a vibrating blade. The "stress ratio" for a mode of vibration is usually defined as the ratio of the maximum vibratory stress in the blade to the strain measured at the gage location multiplied by Young's modulus. The stress ratio is determined from either a finite element analysis of the nominal blade geometry or from laboratory tests and, once determined, is often assumed to be a property that is the same for all blades on the disk. This is a valid assumption if the natural frequency of the mode is well isolated from those of neighboring modes. Modern, low aspect ratio fan and compressor blades behave more like plates than beams and usually have pairs of chordwise, "tip" modes with nearly identical frequencies. When a blade has two modes with nearly the same natural frequencies, the corresponding modes can interact (Yang and Griffin, 1996) and the actual mode shapes can be highly sensitive to small geometric variations that occur during the manufacturing process. As a result, the "stress ratio" for these modes can vary significantly from blade to blade and a single stress ratio no longer provides an accurate method for estimating the maximum stress.

A familiar example of closely spaced modes that illustrates the physics associated with the problem is when the frequency of a primarily bending mode is slightly higher than the frequency of a torsional mode. If a parametric study is conducted in which the chord of the blade is increased it is found that the torsional frequency will tend to increase and, under casual examination, appear to cross the frequency of the bending mode. In fact, under closer inspection one finds that, because the blade is asymmetric (Kim and Griffin, 1994), the frequencies do not cross but veer away from each other. In the veering region, both modes will contain different combinations of the original bending and torsional mode shapes. As the chord of the blade is increased even further, the frequencies emerge from the veering region and the mode shapes have completely switched. This paper focuses on identifying the modal

Presented at the International Gas Turbine & Aeroengine Congress & Exhibition
Orlando, Florida — June 2–June 5, 1997
This paper has been accepted for publication in the Transactions of the ASME
Discussion of it will be accepted at ASME Headquarters until September 30, 1997

content of modes in the veering region since in this case small changes in the blade's geometry due to manufacturing variations can significantly affect their mode shapes.

This paper is organized so as to explain the five concepts that are needed in order to develop a methodology for optimally determining the maximum stress in the case of closely spaced modes. The first is that "nominal" mode shapes from any blade with a representative geometry can be used as a basis for representing the mode shapes in the actual blades. As a result, more than one strain gage measurement must be made on a blade and the resulting information is used to determine the proportions of the "nominal modes" that constitute the modal response in the actual blade. The second concept is associated with establishing how many modes can interact in this manner. LAR blades have such high modal density that three or even four nominal modes might be needed as a basis. These two concepts are presented in section 2.

A problem that arises in implementing this approach is in choosing where to place the strain gages since the actual mode shape can be any combination of two or more nominal modes. The approach presented here is to choose the gage locations so as to minimize the error in the estimate of the maximum stress. Thus, the three remaining concepts are associated with the formulation and development of the optimization problem. In section 3 expressions are development for the error in the stress as caused by placement or gage errors. In section 4, the development of an efficient optimization problem is presented. The approach is illustrated in section 5 using an example from a representative compressor blade. It was found that the standard optimization algorithms for obtaining the optimum gage locations were relatively slow, thus the last concept involves the introduction of a simple, relatively efficient optimization scheme that makes the approach easier to implement.

2. REPRESENTING THE RESPONSE IN TERMS OF NOMINAL MODES

This section deals with the first two concepts developed in this paper. Namely, that the mode shapes in actual blades can be represented as a sum of nominal modes from a representative geometry, and that the number of modes that can interact can be determined from the spacing of the nominal frequencies and the amount of variation in the modal properties of the blade.

2.1 Blade Modes Can be Represented as a Sum of Nominal Modes

In order to motivate this section, consider the following example of the differences in closely spaced tip modes as seen in two nominally identical blades. Figure 1 shows the mode shapes for the two blades that were computed using slightly different finite element models based on their carefully measured geometries. The modes are quite close together, the frequency difference being about 1%. It is clear that the modes for the two blades individually look very different. However, it is clear from even casual observation that each of the modes of blade B has some of the attributes of both of the modes of blade A. In fact, the modes of either blade could be used as a basis to represent the modes of the other blade. The mathematical reason for this result is explained by the following perturbation analysis.

Assume that the "nominal modes" satisfy the structural eigenvalue problem:

$$\mathbf{K}\bar{\phi}_j = \lambda_j \mathbf{M}\bar{\phi}_j \qquad j = 1, 2, \ldots, n \tag{1}$$

where $\mathbf{K}$ and $\mathbf{M}$ are the stiffness and mass matrices of a blade of the nominal geometry,[1] λ_j and $\bar{\phi}_j$ are the eigenvalue and eigenvector associated with the j^{th} mode, and n is the number of degrees of freedom of the system. Similarly, for a manufactured blade, the governing equation can be written as

$$\mathbf{K}'\bar{\phi}'_j = \lambda'_j \mathbf{M}'\bar{\phi}'_j \qquad j = 1, 2, \ldots, n \tag{2}$$

where $\mathbf{K}'$ and $\mathbf{M}'$ are the slightly perturbed stiffness and mass matrices for the actual blade, and λ'_j and $\bar{\phi}'_j$ are the eigenvalue and eigenvector associated with the j^{th} perturbed mode. Assuming perturbations of order δ, where δ is small, the perturbed quantities can be written as:

$$\mathbf{K}' = \mathbf{K} + \delta\mathbf{K}^{(1)} + \delta^2\mathbf{K}^{(2)} + \cdots \tag{3}$$

$$\mathbf{M}' = \mathbf{M} + \delta\mathbf{M}^{(1)} + \delta^2\mathbf{M}^{(2)} + \cdots \tag{4}$$

$$\lambda'_j = \lambda_j + \delta\lambda_j^{(1)} + \delta^2\lambda_j^{(2)} + \cdots \qquad j = 1, 2, \ldots, n \tag{5}$$

[1] Typically, the nominal geometry is either taken from the designer's drawings or may represent the average geometry as measured on a set of manufactured blades.

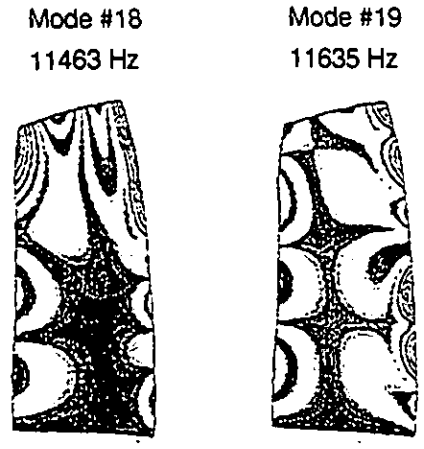

a. Blade A

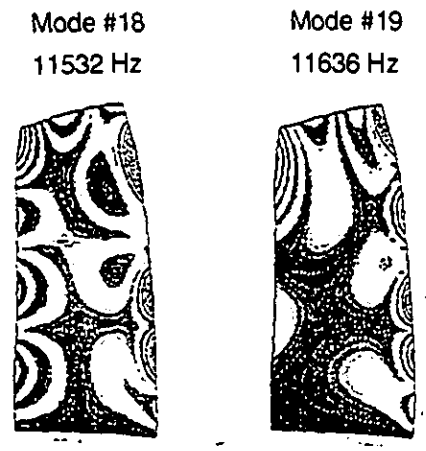

b. Blade B

Figure 1: Tip modes of two blades with slightly different geometries.

$$\bar{\phi}'_j = \bar{\phi}_j + \delta\bar{\phi}_j^{(1)} + \delta^2\bar{\phi}_j^{(2)} + \cdots \qquad j = 1, 2, \ldots, n \tag{6}$$

Substituting (3) through (6) into (2) and equating terms of the same order give the standard results (Meirovitch, 1980)

$$\lambda_j^{(1)} = \frac{\bar{\phi}_j^T\left(\mathbf{K}^{(1)} - \lambda_j\mathbf{M}^{(1)}\right)\bar{\phi}_j}{\bar{\phi}_j^T\mathbf{M}\bar{\phi}_j} \tag{7}$$

$$\bar{\phi}_j^{(1)} = \sum_{i\neq j}\alpha_{ji}^{(1)}\bar{\phi}_i \tag{8}$$

where

$$\alpha_{ji}^{(1)} = \frac{\bar{\phi}_i^T\left(\mathbf{K}^{(1)} - \lambda_j\mathbf{M}^{(1)}\right)\bar{\phi}_j}{\left(\lambda_j - \lambda_i\right)\bar{\phi}_i^T\mathbf{M}\bar{\phi}_i} \qquad i \neq j \tag{9}$$

Equations (8) and (9) imply that, when the unperturbed eigenvalues λ_i and λ_j are well separated, $\bar{\phi}_j^{(1)}$ is of order 1 and the change in the mode shape is small if δ is small. However, when the separation between the eigenvalues is also small, i.e., of order δ, then (9) suggests that $\bar{\phi}_j^{(1)}$ becomes of order $1/\delta$ and the overall change in the mode shape is of order 1. To be more precise, suppose all of the eigenvalues of the unperturbed system are separated by order 1 except for the q clustered eigenvalues λ_{r+1}, λ_{r+2}...., and λ_{r+q} that are separated by order δ. Then it can be shown (Wu, et al., 1995) that $\bar{\phi}'_j$ have the form

$$\bar{\phi}'_j = \begin{cases} \bar{\phi}_j^{(0)} + \delta\bar{\phi}_j^{(1)} + \delta^2\bar{\phi}_j^{(2)} + \cdots & \text{for } j = r+1, \cdots, r+q \\ \bar{\phi}_j + \delta\bar{\phi}_j^{(1)} + \delta^2\bar{\phi}_j^{(2)} + \cdots & \text{otherwise} \end{cases} \tag{10}$$

where

$$\bar{\phi}_j^{(0)} = \sum_{i=r+1}^{r+q}\alpha_{ji}^{(0)}\bar{\phi}_i \qquad j = r+1, \ldots, r+q \tag{11}$$

The $\alpha_{ji}^{(0)}$ are quantities of order 1 that can be determined for specific cases using standard perturbation methods, for example, Yang and Griffin (1996). In summary then, (10) and (11) confirm that when the geometry is slightly perturbed there can be significant mode shape changes (order 1) if the modes are closely spaced and that in this case the perturbed modes can be approximated as a linear combination of the unperturbed closely spaced modes. In terms of modal strains (10) and (11) imply

$$\varepsilon'_i(\bar{y}) = \begin{cases} c_{ii}\,\varepsilon_i(\bar{y}) + O(\delta) & \text{for distinct modes} \\ \sum_{j=r+1}^{r+q} c_{ij}\,\varepsilon_j(\bar{y}) + O(\delta) & \text{for closely spaced modes} \end{cases} \tag{12}$$

where $\bar{y}$ denotes the location and orientation, ε'_i is the strain of the i^{th} perturbed mode, c_{ij} is a coefficient that specifies the amount of the jth unperturbed mode in the i^{th} perturbed mode, ε_j is the strain associated with the j^{th} unperturbed mode. Dropping the i subscript for simplicity, the second equation can be written

$$\varepsilon'(\bar{y}) = \sum_{j=r+1}^{r+q} c_j \varepsilon_j(\bar{y}) + O(\delta) \quad \text{for closely spaced modes} \qquad (13)$$

2.2 The Number of Modes Required for a Basis

The number of nominal modes required for a basis is the number of closely spaced modes that can interact. This number depends on the closeness of the frequencies and the statistical variation that occurs in the modal properties. This problem was investigated in an earlier paper by the authors (Yang and Griffin, 1996). This subsection briefly summarizes the key results from that earlier paper.

It was found that determining whether modes would interact could be established by considering two modes at a time. Two modes would not interact if the fractional frequency difference of the nominal modes was sufficiently large. Specifically, two modes would not interact if

$$\frac{\Delta f}{\bar{f}} > \frac{\sigma\left(k_{ij} - m_{ij}\right)}{2\,\sigma\left(\alpha_{ij}\right)_{\text{allowable}}}$$

where $\sigma(\bullet)$ denotes a standard deviation, Δf is the frequency difference, $\bar{f}$ is the mean frequency, and k_{ij} and m_{ij} are parameters associated with i^{th} and j^{th} modes in the normalized modal stiffness and mass matrices. The term α_{ij} is the modal contribution from i^{th} unperturbed mode to j^{th} perturbed mode.

The standard deviation in the modal parameters can be calculated using a finite element program and the method described in the referenced paper if the variations in the geometries of manufactured blades are carefully measured for a particular blade design. For example, it was found by the authors that, for a representative LAR compressor blade, all values of $\sigma(k_{ij} - m_{ij})$ for the first thirty modes were less than 0.005. If the allowable standard deviation of modal interaction

$$\sigma\left(\alpha_{ij}\right)_{\text{allowable}}$$

is 5%, then two modes would not significantly interact if their frequency difference is greater than 5%. Consequently, for this blade, a mode calculated from the nominal geometry with a frequency that is separated from its neighbors by more than 5% can be treated as an isolated mode and a single stress ratio can be used to interpret strain gage data. Alternatively, if a mode is not isolated then all nominal modes within 5% of its frequency must be used as a basis in determining its behavior.

3. DETERMINING THE ERROR IN THE ESTIMATE OF MAXIMUM STRESS

In the case of closely spaced modes, the mode shape in the actual blade is unknown except for the fact that it is some linear combination of the closely spaced nominal modes. The goal of the measurements is to determine the amount of each constitutive mode present and use the information to calculate the maximum stress in the blade. Consequently, the objective of the optimization process is to place the strain gages so that any errors in the strain measurements have a minimal effect on the calculation of the maximum stress.

First, a procedure will be described for calculating the maximum stress in the blade under the assumption that there are no strain gage errors. The resulting equations will then be used to establish expressions for the error in the maximum stress that results when measurement errors are introduced.

3.1 Expressions for the Maximum Stress

From (13), it is clear that strain measurements at multiple points on the actual (perturbed) blade have to be taken in order to resolve the modal content of the perturbed mode, i.e., determine c_j by solving the equations,

$$\varepsilon'(\bar{x}_i) = \sum_{j=r+1}^{r+q} c_j \varepsilon_j(\bar{x}_i) \qquad i = 1, 2, \ldots, m \qquad (14)$$

where $\bar{x}_i$ represents the location and orientation of the i^{th} gage and m is the number of gages. Terms of Order δ are small and have been dropped. (They could be treated in a manner similar to gage errors as described in the following sections.) Alternatively, (14) can be recast in a matrix form,

$$\bar{\varepsilon}'(\bar{x}) = \mathbf{E}(\bar{x})\,\bar{c} \qquad (15)$$

where

$$\bar{x} = \left[\bar{x}_1^T, \bar{x}_2^T, \cdots, \bar{x}_m^T\right]^T \qquad (16)$$

$$\bar{\varepsilon}'(\bar{x}) = \left[\varepsilon'(\bar{x}_1), \varepsilon'(\bar{x}_2), \cdots, \varepsilon'(\bar{x}_m)\right]^T \qquad (17)$$

$$\mathbf{E}(\vec{x}) = \begin{bmatrix} \varepsilon_{r+1}(\vec{x}_1) & \cdots & \varepsilon_{r+q}(\vec{x}_1) \\ \vdots & \ddots & \vdots \\ \varepsilon_{r+1}(\vec{x}_m) & \cdots & \varepsilon_{r+q}(\vec{x}_m) \end{bmatrix} \tag{18}$$

$$\vec{c} = \left[c_{r+1}, c_{r+2}, \cdots, c_{r+q}\right]^T \tag{19}$$

From (15), the least square fit solution for $\vec{c}$ is

$$\vec{c} = \mathbf{E}^+(\vec{x})\vec{\varepsilon}'(\vec{x}) \tag{20}$$

where $m \geq q$ and $\mathbf{E}^+$ is the generalized inverse of $\mathbf{E}$ (Ben-Israel and Greville, 1974) with the following expression

$$\mathbf{E}^+ = \left(\mathbf{E}^T\mathbf{E}\right)^{-1}\mathbf{E}^T \tag{21}$$

For the ideal case in which there are no measurement errors, (20) simply provides an exact solution. Notice that, when $m = q$, $\mathbf{E}^+$ will simply become $\mathbf{E}^{-1}$.

Now, once the modal content $\vec{c}$ is known, the stress at any location and orientation $\vec{y}$ can be readily calculated

$$\sigma'(\vec{y}) = \sum_{j=r+1}^{r+q} c_j \sigma_j(\vec{y}) \tag{22}$$

where σ' is the stress of the perturbed mode and σ_j is the modal stress associated with the j^{th} unperturbed mode. Writing (22) in a matrix form,

$$\sigma'(\vec{y}) = \vec{\sigma}^T(\vec{y})\vec{c} \tag{23}$$

where

$$\vec{\sigma}(\vec{y}) = \left[\sigma_{r+1}(\vec{y}), \sigma_{r+2}(\vec{y}), \cdots, \sigma_{r+q}(\vec{y})\right]^T \tag{24}$$

and substituting (20) into (23), the stress of the perturbed mode for a given location and orientation $\vec{y}$ is

$$\sigma'(\vec{y}) = \vec{\sigma}^T(\vec{y})\mathbf{E}^+(\vec{x})\vec{\varepsilon}'(\vec{x}) \tag{25}$$

Thus, given strain measurements of the perturbed mode from m gages ($\vec{\varepsilon}'$) and the strains of the q unperturbed modes corresponding to the gage locations and orientations ($\mathbf{E}$), (25) calculates the modal stress of the perturbed mode. However, if the gage placements are poorly chosen, the inaccuracies in placements and gages can be significantly magnified. In the following sections, an error estimate will be developed from (25) so that the optimal placements for gages can be found by minimizing the error in the modal stresses.

3.2 Stress Errors Caused by Measurement Errors

The errors in strain measurements $\Delta\vec{\varepsilon}'$ are caused by gage placement errors $\Delta\vec{x}$ and gage errors $\Delta\vec{g}$. According to (15), they have the following relation,

$$\vec{\varepsilon}'(\vec{x}) + \Delta\vec{\varepsilon}' = \mathbf{E}(\vec{x} + \Delta\vec{x})\vec{c} + \Delta\vec{g} \tag{26}$$

However, since $\Delta\vec{x}$ and $\Delta\vec{g}$ are not known when the strains are measured, (15) is used to infer the modal content under the assumption that there are no measurement errors. As a result, all of the measurement errors generate an error in the modal content $\Delta\vec{c}$ where

$$\vec{\varepsilon}'(\vec{x}) + \Delta\vec{\varepsilon}' = \mathbf{E}(\vec{x})\left(\vec{c} + \Delta\vec{c}\right) \tag{27}$$

By equating the right-hand side of (26) and (27) and solving for $\Delta\vec{c}$

$$\Delta\vec{c} = \mathbf{E}^+(\vec{x})\left\{\left[\mathbf{E}(\vec{x} + \Delta\vec{x}) - \mathbf{E}(\vec{x})\right]\vec{c} + \Delta\vec{g}\right\} \tag{28}$$

Equation (28) provides an error estimate for the modal content. Now, since (23) with errors can be written as

$$\sigma'(\vec{y}) + \Delta\sigma' = \vec{\sigma}^T(\vec{y})\left(\vec{c} + \Delta\vec{c}\right) \tag{29}$$

where $\Delta\sigma'$ is the error in the stress of the perturbed mode. Subtracting (23) from (29) implies

$$\Delta\sigma' = \vec{\sigma}^T(\vec{y})\,\Delta\vec{c} \tag{30}$$

Substituting (28) into (30) implies

$$\Delta\sigma' = \vec{\sigma}^T(\vec{y})\mathbf{E}^+(\vec{x})\left\{\left[\mathbf{E}(\vec{x} + \Delta\vec{x}) - \mathbf{E}(\vec{x})\right]\vec{c} + \Delta\vec{g}\right\} \tag{31}$$

Equation (31) is the error estimate for the calculated stress of the perturbed mode in terms of gage placement error and gage error.

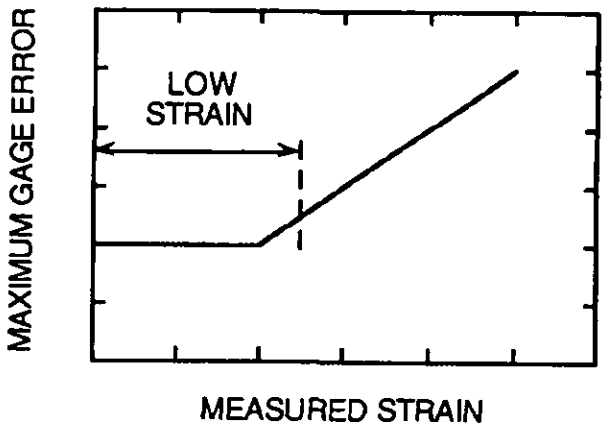

a. Approximated by a bilinear curve

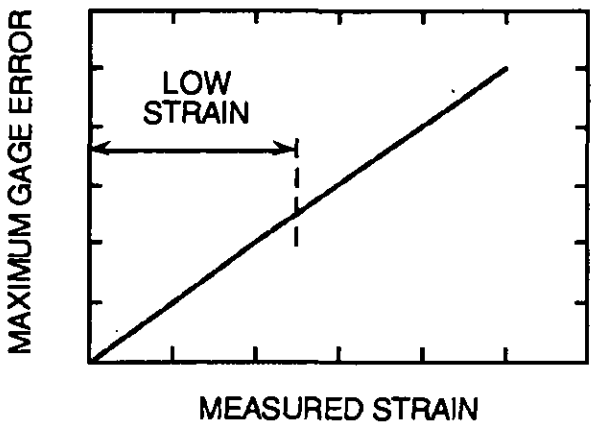

b. Approximated by a straight line

Figure 2: Maximum Gage Error as a Function of Measured Strain

4. OPTIMIZATION PROBLEM

4.1 Statement of the Problem

An initial statement of the optimization problem would be to choose the placement of the gages $\bar{x}$ so as to minimize the error in the maximum stress as determined by equation (31). The optimization process would have to consider all possible values of $\bar{c}$, $\bar{x}$, $\Delta\bar{x}$, and $\Delta\bar{g}$. Further complications are that the maximum stress location $\bar{y}_{max}$ would change with the modal content $\bar{c}$ and that the gage error could be a nonlinear function of strain which in turn is a function of the gage location and the modal content. Consequently, this initial statement of the optimization problem is too complex and would result in prohibitive computational costs. Thus, a number of simplifications are introduced to make the problem tractable and provide a practical engineering solution.

4.2 Linearized Strain Gage Error

Strain gage error is, in general, a nonlinear function of strain. One reason for this is that there is a threshold value of strain below which it is difficult to measure. In addition, there will be an error in the gage's calibration constant which results in an error proportional to the strain. Thus, the gage error might be approximated by a bi-linear curve as depicted in Figure 2(a). The nonlinear nature of the error makes the optimization process far more costly. From a practical point of view, the threshold error means that gages should not be placed in areas of low stress since the percentage error in the measurements would be large. The approach used in this paper is to assume that the strain gage error is linear (Figure 2(b)) and to have a separate optimization criterion that the strain gages will not be placed in low strain areas, i.e., candidate strain gage locations must satisfy the condition that

$$\frac{\text{modal strain}}{\text{maximum modal strain}} > \beta \qquad (32)$$

for all constituent modes, where β, the cutoff ratio, is less than 1 and is specified by the user. Assume $\Delta\bar{g}$ is linear in $\bar{\varepsilon}'$ over the range of interest, then

$$\Delta\bar{g} \equiv \Delta\mathbf{G}\,\bar{\varepsilon}' \qquad (33)$$

where $\Delta\mathbf{G} = \text{diag}(\Delta G_1, \Delta G_2, \cdots, \Delta G_m)$ and ΔG_i is the ratio of the gage error to the actual strain at the i^{th} gage. Then, by substituting (15) in (33) and including the placement error $\Delta\bar{x}$, the following relationship is obtained

$$\Delta\bar{g} = \Delta\mathbf{G}\,\mathbf{E}(\bar{x} + \Delta\bar{x})\,\bar{c} \qquad (34)$$

Substituting (34) in (31), implies

$$\Delta\sigma' = \bar{\sigma}^T(\bar{y})\,\mathbf{E}^+(\bar{x})\left[\,\mathbf{E}(\bar{x} + \Delta\bar{x}) - \mathbf{E}(\bar{x}) + \Delta\mathbf{G}\,\mathbf{E}(\bar{x} + \Delta\bar{x})\,\right]\bar{c} \qquad (35)$$

The advantage of using (35) instead of (31) is that the magnitude of $\bar{c}$ can be eliminated from the simulation and only the "orientation" of $\bar{c}$ needs to be considered.

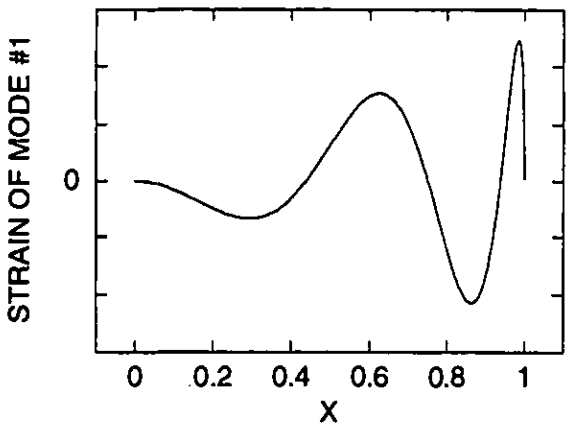

a. Mode #1

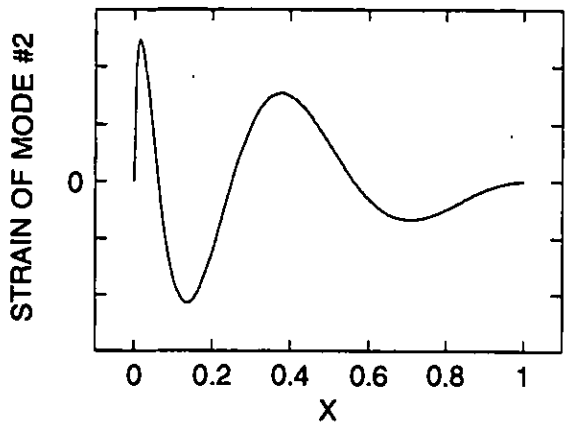

b. Mode #2

Figure 3: Strains of One-dimensional Localized "Tip Modes"

4.3 Use a matrix norm to minimize $\Delta\bar{c}$ instead of $\Delta\sigma'(\bar{y}_{max})$

Substituting (34) in (28), results in

$$\Delta\bar{c} = \mathbf{E}^{+}(\bar{x})\left[\, \mathbf{E}(\bar{x}+\Delta\bar{x}) - \mathbf{E}(\bar{x}) + \Delta\mathbf{G}\,\mathbf{E}(\bar{x}+\Delta\bar{x}) \,\right]\bar{c} \quad (36)$$

Using "norms", (36) implies that the fractional error in the modal content has an upper bound, i.e.,

$$\frac{\| \Delta\bar{c} \|}{\| \bar{c} \|} \le \| \mathbf{M} \| \quad (37)$$

where

$$\mathbf{M} = \mathbf{E}^{+}(\bar{x})\left[\, \mathbf{E}(\bar{x}+\Delta\bar{x}) - \mathbf{E}(\bar{x}) + \Delta\mathbf{G}\,\mathbf{E}(\bar{x}+\Delta\bar{x}) \,\right] \quad (38)$$

Thus, the upper bound on the fractional error in the modal content can be optimized by minimizing the norm of $\mathbf{M}$ for all $\Delta\bar{x}$ and $\Delta\mathbf{G}$ within certain prescribed physical limits. The advantage of using (37) to minimize $\| \Delta\bar{c} \| / \| \bar{c} \|$ instead of using (35) to minimize $\Delta\bar{\sigma}$ at $\bar{y}_{max}$ is that the search of $\bar{y}_{max}$ for each orientation of $\bar{c}$ is eliminated as well as simulating the orientation of $\bar{c}$ from the optimization process.

The potential difficulty in using norms is that it may provide a highly conservative bound on the error and may not result in an optimal choice of gage placements. This issue is explored in the following one dimensional, two mode case study. The nominal mode shapes shown in Figure 3 were chosen to have the characteristics of typical tip modes, i.e., the high strain regions are highly localized (Balaji and Griffin, 1995). First, an exhaustive parametric study was conducted for specific placement and gage errors in which the error in the maximum stress was calculated as a function of the two strain gage locations x_1 and x_2 for all possible ratios of c_2 to c_1. The maximum error is plotted as a function of gage position in Figure 4(a). Then $\| \mathbf{M} \|$ is plotted as a function of gage location in Figure 4(b).[2] From the figures, it is clear that both quantities exhibit similar trends and, consequently, a minimum of one quantity is approximately a minimum of the other. In fact, a minimization of the error in the stress resulted in an optimum gage location $\bar{x}$ = (0.37, 0.86), a maximum stress error of 12.7%, and a value of $\| \mathbf{M} \|$ equal to 22.9%. A minimization of $\| \mathbf{M} \|$ resulted in an optimum gage location $\bar{x}$ = (0.14, 0.87), a value of $\| \mathbf{M} \|$ equal to 20.7%, and a maximum stress error of 13.2%. From an expense point of view, minimizing $\| \mathbf{M} \|$ was a factor of 30 more efficient while producing satisfactory results. The improvement in efficiency would be even larger for more realistic applications.

4.4 Linearize $\| \mathbf{M} \|$

Computational efficiency can be further improved by linearizing the expressions for $\mathbf{M}$. For small $\Delta\mathbf{G}$ and $\Delta\bar{x}$, (38) implies the first order approximation of $\mathbf{M}$ is

$$\mathbf{M}(\bar{x}, \Delta\mathbf{G}, \Delta\bar{x}) \cong \mathbf{M}_g(\bar{x}, \Delta\mathbf{G}) + \mathbf{M}_x(\bar{x}, \Delta\bar{x}) \quad (39)$$

where

[2] The infinity norm is used in this research.

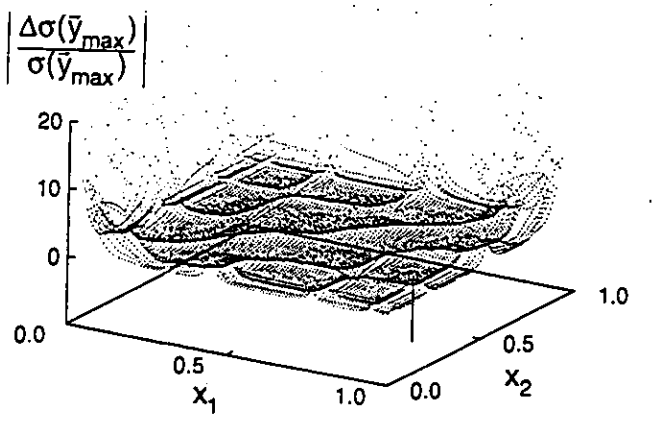

a. Percentage error of maximum stress

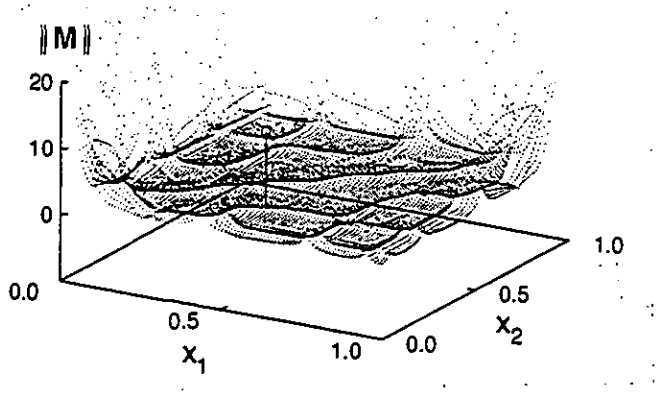

b. Upper board of percentage error of modal content (eq. (37))

Figure 4: Comparison of Two Different Optimization Indices. The squares indicate the global minimums.

$$\mathbf{M}_g(\bar{x}, \Delta\mathbf{G}) = \mathbf{E}^+(\bar{x})\,\Delta\mathbf{G}\,\mathbf{E}(\bar{x}) \tag{40}$$

$$\mathbf{M}_x(\bar{x}, \Delta\bar{x}) = \mathbf{E}^+(\bar{x})\,\mathbf{E}(\bar{x} + \Delta\bar{x}) - \mathbf{I} \tag{41}$$

(39) implies that

$$\|\mathbf{M}(\bar{x}, \Delta\mathbf{G}, \Delta\bar{x})\| \le \|\mathbf{M}_g(\bar{x}, \Delta\mathbf{G})\| + \|\mathbf{M}_x(\bar{x}, \Delta\bar{x})\| \tag{42}$$

Substituting (42) in (37), we have

$$\frac{\|\Delta\bar{c}\|}{\|\bar{c}\|} \le \|\mathbf{M}\| \le \|\mathbf{M}_g\| + \|\mathbf{M}_x\| \tag{43}$$

The advantage of using (43) is that it decouples $\Delta\mathbf{G}$ and $\Delta\bar{x}$ effects, thus reducing the number of combinations that need to be considered in the simulations. In addition, since the extremes of linear functions are at the "end points," only the errors associated with the "end points" have to be calculated.

5. CASE STUDY AND OPTIMIZATION METHODS

The two modes depicted in Figure 1 were calculated from a two dimensional finite element model of a representative modern compressor blade. Because their frequencies are quite close they interact significantly and consequently provide an interesting example of the optimization process.

A 40 by 40 mesh was used to model the airfoil (Figure 5). To further simplify the calculations, the gages were assumed to be located at the centers of elements. Thus, 1600 possible gage locations had to be considered for each of the two strain gages. In addition, the orientation of the gages also had to be specified for each location. Orientations of 0° to 180° at intervals of 15° were simulated. A gage orientation error of plus or minus 5° and gage error of 5% were assumed.

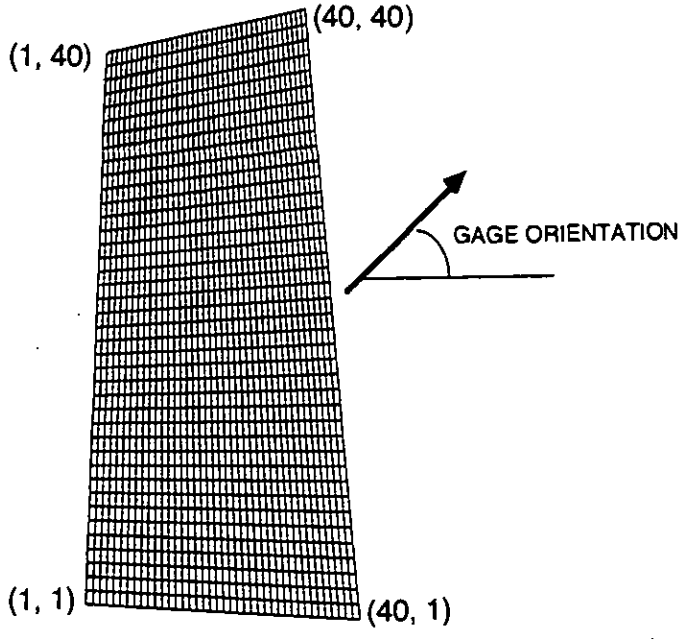

Figure 5: Finite Element Model of a Two-dimensional Simplified Blade

5.1 Alternating Optimization and Simulated Annealing Compared with Benchmark

As indicated in Figure 4, the gage placement optimization problem exhibits a number of local minima in terms of multiple variables.[3] An optimization procedure based on simulated annealing was utilized to find the optimum gage locations since simulated annealing has a well established reputation for efficiently solving problems of this type (Press, et al., 1992). In order to first validate the optimization program, the simulated annealing solution was compared with results from an "exact solution" of a simplified test problem. The exact solution was found using an exhaustive search of the parameter space. To make the problem more tractable for the exhaustive search, only gage orientation errors and gage error were simulated. The cutoff ratio β (section 4.2) was assumed to be zero.

The simulated annealing procedure gave the same global minimum as the exhaustive search, i.e., if the gages were optimally placed, then one gage should be located at (12, 27, 75°) and the second gage at (37, 5, 60°), where the first two numbers specify the location of the element (column and row) and the third the orientation of the gage. For the optimum gage arrangement, γ_M = 7.4% where γ_M denotes $\|\mathbf{M}_g\| + \|\mathbf{M}_x\|$ as in equation (43).

The exhaustive search computer program ran for 11 hours on an IBM RISC 6000 workstation. The simulated annealing algorithm took an order of magnitude less time (1 hour) to find the same global minimum. Even though the simulated annealing program was much faster than an exhaustive search, it was still a relatively slow procedure — especially if gage location errors were included in addition to gage orientation errors.[4] In order to make the optimization procedure efficient a new simple optimization procedure was developed that seems to work quite well for the gage optimization problem.

Upon examination of the data it was found that the optimum gage locations could usually be found by optimizing one strain gage location at a time. More specifically, first arbitrarily fix the location of the first gage and minimize γ_M by an exhaustive search on the orientation and location of gage 2 and the orientation of gage 1. Then repeat the process with the location of the second gage fixed at its optimized location. Continue to alternate until the procedure converges.

It should be noted that this procedure sometimes results in local minima. Therefore, several runs using different guesses of gage one's initial location should be made and the one with the lowest local minimum taken as an approximation of global optimum. When this "alternating optimization" approach was used to solve the benchmark problem, it took approximately 12 seconds per initial guess to find a converged solution. In the majority of cases the procedure, in fact, converged to the global optimum. Consequently, even with multiple initial guesses the alternating optimization procedure was an order of magnitude faster than simulated annealing .

5.2 Full Simulation: Effect of β on Error and Computation Time

A complete simulation that included gage location errors as well as orientation and gage errors was performed using alternating optimization. The resolution for gage orientation was 15° and for gage placement was one element. The maximum error in the orientation and placement of the gages was also set at 5° and one element and the gage error at 5%. The initial position of gage one was varied using nine different values corresponding to three by three grid in the airfoil. The algorithm converged to the same optimum in every case. Once the optimum strain gage locations were determined that would minimize the norm of $\mathbf{M}$ as established by equation (43), then the maximum error in modal content and in the maximum stress were calculated, i.e.,

$$\gamma_c \equiv \max_{\|\bar{c}\|=1} \frac{\|\Delta\bar{c}\|}{\|\bar{c}\|} \tag{44}$$

$$\gamma_\sigma \equiv \max_{\|\bar{c}\|=1} \left| \frac{\Delta\sigma'(\bar{y}_{max})}{\sigma'(\bar{y}_{max})} \right| \tag{45}$$

where $\bar{y}_{max}$, determined by modal content $\bar{c}$, is the location and orientation where the maximum stress occurs. The values of γ_c and γ_σ were evaluated by checking 36 uniformly distributed $\bar{c}$'s on the unit circle $\|\bar{c}\| = 1$.

The results of simulations for various cut-off ratios β are shown in the first three columns of Table 1. Recall that the purpose of the cut-off ratio is that it prevents placing strain gages in locations where the strains in the nominal

---

3 As a result, linear programming methods are not appropriate for this problem.

4 Because of its two dimensional nature, four extreme location errors have to be considered in the simulation. Location errors of one gage combined with those of the other gage will increase the computation costs by a factor of sixteen.

modes are too small. An examination of Table 1 reveals several interesting results. The first is that the amount of computing time decreases as β increases since fewer strain gage locations need to be considered in the optimization. Although it appears that the errors will be larger for larger values of β, in fact, the simulations do not include the effect of the larger percentage gage error that occurs for low strain measurements. Thus, the placement of the strain gages that result from a larger value of β may well correspond to a lower actual error. The second result is the degree to which the value of γ_M provides a reasonable estimate of γ_c and γ_σ, the maximum error in the modal content and in the maximum stress. The fact that γ_M is smaller than γ_c in two of the cases is surprising since the norm of $\mathbf{M}$ should provide an upper bound on γ_c. Recall that the norm of $\mathbf{M}$ did provide an upper bound on γ_c in the case study discussed in section 4.3. However, the γ_M used in this section utilizes the approach given in section 4.4 and is only a linearized approximation of the norm of $\mathbf{M}$. The use of a linearized estimate of the norm significantly increases computational efficiency at the expense of losing the strict results that $\gamma_c \leq \gamma_M$. However, it is clear from the results that γ_M still provides a reasonable estimate of the maximum errors in the modal content and the maximum stress.

Table 1: Comparison of Optimized Gage Placements Derived From Different β and an Aribitrary Gage Placement

Cutoff Ratio β	0%	25%	35%	—
CPU Time (mins.)	25.2	14.6	9.3	—
Gage 1 Location	(13, 40)	(13, 40)	(11, 39)	(37, 1)
Gage 1 Orientation	150°	150°	150°	45°
Gage 2 Location	(40, 1)	(40, 1)	(40, 1)	(6, 5)
Gage 2 Orientation	45°	45°	45°	75°
γ_M	14.5%	14.5%	20.1%	30.6%
γ_c	14.7%	14.7%	18.9%	29.3%
γ_σ	13.7%	13.7%	15.7%	28.3%

The last column of Table 1 shows representative results that would occur if the gages were placed in arbitrary locations. For this case, the error that could occur in the maximum stress is almost twice as large as for the optimal case. In fact, by maximizing γ_M, it is possible to find gage locations that would result in much larger errors. Consequently, the optimization of gage placement and orientation can significantly reduce the amount of error that can occur in determining the maximum stress in closely spaced modes.

6. CONCLUSIONS

Modern, low aspect ratio blades often have closely spaced, high frequency "tip" modes that are sensitive to the slight changes in the blade's geometry that can occur during the manufacturing process. From perturbation analyses, it is known that the modes that occur in the actual blades can be approximated as a linear combination of the unperturbed modes, i.e., the modes that occur in a blade with a nominal geometry. This suggests that stresses in the actual blades can be estimated by making multiple strain measurements and inferring the modal content of the constituent modes. If this effect is not taken into account, then the mode may be incorrectly identified — a mistake that could result in extremely large errors in the estimated stresses.

A current procedure that may be used is to perform a complete experimental stress survey on closely spaced modes and establish different stress ratios for every instrumented blade. A problem with this approach is that it is quite expensive and may not work since these modes are very sensitive to small changes in the structural properties and the properties are changed by the speed of the engine. As a result, the process of rotating the blade may cause closely spaced frequencies to change and even switch in order. Thus, the results of the stress survey may not be applicable under engine operating conditions.

Once it is understood that the modal content of the actual response needs to be determined by multiple strain measurements then the location and orientation of the gages have to be carefully selected since a poor choice can significantly amplify any gage or placement errors. The procedure for optimizing the location of the strain gages is made significantly more complicated by the fact that the actual mode shape is known only to the extent that it is a linear combination of the nominal modes. A procedure was discussed for determining how many nominal modes are required as a basis. Then, mathematical expressions were developed for the error in the maximum stress as a function of the gage and placement errors. The formulation was then simplified through the use of matrix norms and various linearizations in order to make the problem more computationally tractable.

Several test problems were solved in order to validate and illustrate the approach and a new optimization procedure was introduced that significantly reduced computation times. It was shown that the optimal selection of gage locations could reduce the error in the estimate of the maximum stress by at least a factor of two. Thus, a theory and methodology have been developed and demonstrated for optimally measuring the maximum stress that occurs in closely spaced modes.

REFERENCES

Balaji, G. and Griffin, J.H., 1995, "The Resonant Response of a Tapered Beam and Its Implications to Blade Vibration," ASME paper 95-GT-453, accepted for publication in the Journal of Engineering for Gas Turbines and Power, Transactions of the ASME.

Ben-Israel, A. and Greville, T.N.E., 1974, *Generalized Inverses: Theory and Applications*, New York: Wiley.

Kim, N. and Griffin, J.H., 1994, "Sensitivity of Bonded and Composite Beams," *Journal of Sound and Vibration*, Vol. 177, pp. 71-92.

Meirovitch, L. 1980, *Computational Methods in Structural Dynamics*, Alphen aan den Rijn, The Netherlands; Rockville, MD: Sijthoff & Noordhoff.

Press, W.H., Teukolsky, S.A., Vetterling, W.T., and Flannery, B.P., 1992, *Numerical Recipes in C, The Art of Scientific Computing, 2nd Ed.*, New York: Cambridge University Press.

Wu, W.-T., Griffin, J.H., and Wickert, J.A., 1995, "Perturbation Method for the Floquet Eigenvalues and Stability Boundary of Periodic Linear Systems," *Journal of Sound and Vibration*, Vol. 182, pp. 245-257.

Yang, M.-T. and Griffin, J.H., 1996, "A Normalized Modal Eigenvalue Approach for Resolving Modal Interaction," ASME paper 96-GT-111, accepted for publication in the Journal of Engineering for Gas Turbines and Power, Transactions of the ASME.